J.T. WEAVER, B.V. LE QUANG AND G. FISCHER

Remarks on the comparison of analytical and numerical model calculations

Many programs now exist for computing numerically the electromagnetic response of two-dimensional conductivity structures in the Earth to an external, time-varying magnetic source. In most cases, as in this paper, the magnetic source is assumed to be uniform, horizontal and harmonic in time with period $T = 2\pi/\omega$. A comparison of the numerical results given by these methods applied to several pre-assigned models is currently being organised by Professor M.S. Zhdanov of Moscow under the project name COMMEMI.

At the Observatoire Cantonal we believe that in addition to making this numerical comparison it is desirable, if not essential, to develop some simple "control models" for which analytic solutions are available. Any numerical procedure should at least be shown to give acceptable agreement with these analytic solutions before being subjected to a comparison with other numerical methods. After all, if three different computer programs happen to give three different sets of results for any of the proposed numerical models in the COMMEMI project then there is no knowing which of these programs is the most accurate unless analytic control solutions are also available.

To our knowledge the only detailed investigation of this nature to have been undertaken previously is described in the Diplomarbeit of Klügel (1976). In that work the results given by the finite difference program of Dr. W. Müller (see Losecke and Müller, 1975) were compared with the classical H-polarisation solution obtained by d'Erceville and Kunetz (1962) for the two-plate model – actually Klügel took the thickness of the plates to be several skin-depths so that he was effectively considering the quarter-space model shown in Fig. 1a. The corresponding finite difference calculations for an E-polarisation field were compared with what can be called a "quasi-analytic" solution of the two-plate model based on a method of successive approximations first proposed by Weidelt (1966).

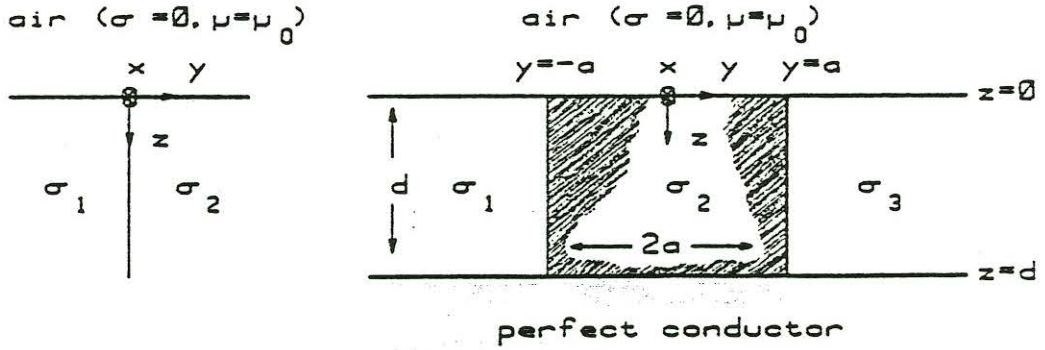

(a) (b)

Fig. 1

In our opinion the "control model" shown in Fig. 1b is a somewhat better one to use for the following reasons:

(i) It includes such well-known models as the dike ($\sigma_1 = \sigma_3$), the vertical fault ($\sigma_2 = \sigma_3$), and the quarter-space ($\sigma_2 = \sigma_3$, $d \to \infty$) as special cases.

(ii) The effect of both high and low conductivity contrasts can be examined in the same model by choosing (say) $\sigma_2/\sigma_1 \geq 10$, $1 < \sigma_2/\sigma_3 < 5$.

(iii) Programs which can only handle "anomalous" regions of finite horizontal extent embedded in a "normal" one-dimensional structure can also be tested by putting $\sigma_1 = \sigma_3$ in the control model.

(iv) With $\sigma_1 < \sigma_2 < \sigma_3$ (or $\sigma_1 > \sigma_2 > \sigma_3$), and a chosen small so that $2a = h$, where h is the node separation in the numerical grid, the control model can be used to check the accuracy of the numerical solution for a model in which the conductivity changes gradually from one value (σ_1) to the next (σ_3) over a transition zone comprising three successive cells – normally only simple conductivity contrasts can be considered.

(v) The perfect conductor at finite depth d provides a clean cut-

off to the numerical model and permits the use of a reasonably small grid (with consequent savings in CPU time) when testing programs against the control model.

A similar model, called the "segmented overburden" by Wait (1982), in which the basement is a perfect insulator rather than a perfect conductor, has been solved analytically for H-polarisation induction by Wait and Spies (1974). A closed solution is possible in this polarisation because the spatial part of the magnetic field external to the Earth is then uniform and horizontal everywhere, thus providing the simple boundary condition $B_x(y,0) = B_o$ (const) on the surface z = 0. The H-polarisation solution for the control model shown in Fig. 1b can be obtained in a similar manner by making the appropriate change of boundary condition at z = d to account for the perfect conductor. The solution for the magnetic field (with a time factor exp(iωt) understood and the permeability taken as μ_o everywhere) is then found to be

$$B_x(y,z) = \begin{cases} B_1 & (y < -a) \\ B_2 & (|y| \leq a) \\ B_3 & (y > a) \end{cases}$$

where for i = 1,2,3

$$\frac{B_i}{B_o} = \frac{\cosh[(d-z)\alpha_i\sqrt{i}]}{\cosh(d\alpha_i\sqrt{i})} + \sum_{m=0}^{\infty} F_m^{(i)}(y)\sin(k_m z) \qquad (1)$$

with

$$\alpha_i = \sqrt{\omega\mu_o\sigma_i}\ , \qquad k_m = (2m+1)\pi/2d\ , \qquad \gamma_m^{(i)} = \sqrt{k_m^2 + i\alpha_i^2}\ ,$$

and

$$F_m^{(1)}(y) = \beta_m^{(1)} A_m^{(1)} e^{\gamma_m^{(1)}(a+y)}\ ,$$

$$F_m^{(3)}(y) = \beta_m^{(3)} A_m^{(3)} e^{\gamma_m^{(3)}(a-y)}\ ,$$

$$F_m^{(2)}(y) = (A_m^{(1)} - C_m^{(1)}) e^{\gamma_m^{(2)}(a+y)} + (A_m^{(3)} - C_m^{(3)}) e^{\gamma_m^{(2)}(a-y)}.$$

Here we have defined for i = 1,3

$$A_m^{(i)} = \{2e^{-2a\gamma_m^{(2)}} \bar{K}_m^{(i)} - [\,1 + \bar{\beta}_m^{(i)} + (1-\bar{\beta}_m^{(i)}) e^{-4a\gamma_m^{(2)}}]K_m^{(i)}\}/D_m,$$

$$C_m^{(i)} = \{(1 - \beta_m^{(i)})e^{-2a\gamma_m^{(2)}}\bar{K}_m^{(i)} - (1 + \bar{\beta}_m^{(i)})K_m^{(i)}\}/D_m \quad ,$$

where

$$\beta_m^{(i)} = \frac{\gamma_m^{(2)}/\sigma_2}{\gamma_m^{(i)}/\sigma_i} \quad , \qquad K_m^{(i)} = \frac{2ik_m(\alpha_2^2 - \alpha_i^2)}{\{\gamma_m^{(2)}\gamma_m^{(i)}\}^2} \quad ,$$

$$\bar{\beta}_m^{(i)} = \beta_m^{(1)}\beta_m^{(3)}/\beta_m^{(i)} \quad , \qquad \bar{K}_m^{(i)} = K_m^{(1)}K_m^{(3)}/K_m^{(i)} \quad ,$$

and

$$D_m = (1 + \beta_m^{(1)})(1 + \beta_m^{(3)}) - (1 - \beta_m^{(1)})(1 - \beta_m^{(3)})e^{-4a\gamma_m^{(2)}} \quad .$$

The derived field components E_y and E_z can be obtained from (1) by differentiation according to Maxwell's equations.

The field values given by this analytic solution for the model parameters σ_1 = 0.1 S/m, σ_2 = 1.0 S/m, σ_3 = 0.5 S/m, a = 10 km, d = 50 km, T = 300 s have been compared with the corresponding numerical results given by (i) the finite difference program of Brewitt-Taylor and Weaver (1976) together with some (unpublished) improvements in the method for calculating the derived fields and (ii) the finite element program of Kisak and Silvester (1975). It should be noted that the skin-depths in the three regions from left to right are respectively 27.6 km, 8.7 km and 12.3 km so that the width of the central segment is only just over two skin-depths while the thickness of the left segment is under two skin-depths. For the finite difference calculation we used a 35 x 16 grid with nodes at the points y = -130, -110, -90, -80, -70, -61, -52, -43, -34, -25, -19, -15, -12, -10, -8.5, -7, -5, -2.5, 0, 2.5, 5, 7, 8.5, 10, 12, 15, 18, 22, 26, 30, 34, 38, 43, 50 and 60 km, and z = 0, 1.5, 3, 5, 7.5, 10, 12.5, 15, 17.5, 20, 24, 28, 32, 40, 45 and 50 km. For the application of the finite element program the region $z \geq 0$, -130 km < y < 60 km was divided into the triangular elements shown in Fig. 2 (N.B. this figure also shows a strip in the air region $z < 0$ divided into the triangular elements used for E-polarisation calculations). The CPU time required for these calculations was 50 s with the finite difference program and 90 s with the finite element program, on a VAX-780 computer.

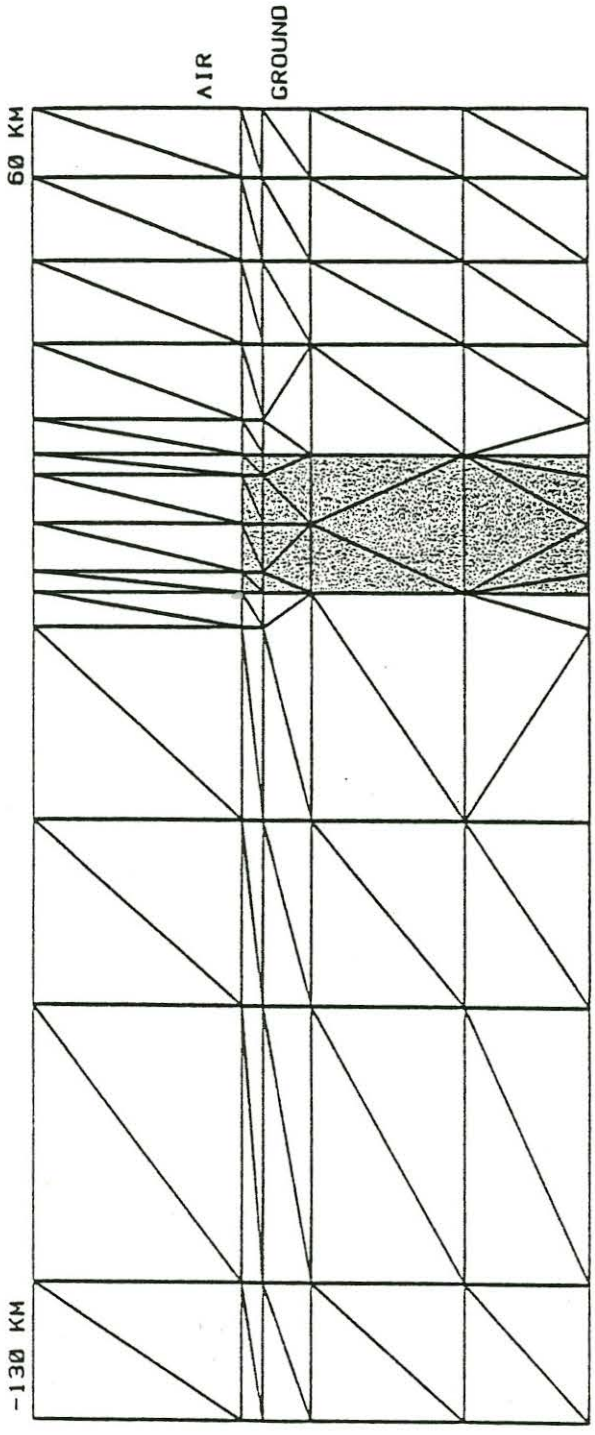
FINITE ELEMENT - KISAK SILVESTER - E POL 300 SEC
AIR
GROUND
60 KM
-130 KM

Fig. 2

Fig. 3 compares the variation of the real and imaginary parts of the horizontal electric field E_y (normalised by B_o) across the surface of the conductor. A visual inspection of the graphs indicates that the agreement between the finite difference calculations and the analytic solution is excellent. In fact the errors were limited to the range 1% - 4%. The finite element calculations are not quite so satisfactory. The field values for $y > -10$ km are in reasonably good agreement with the analytic results, but some discrepancies occur over the region of least conductivity $y < -10$km. The variation of the field there is less smooth and errors greater than 10% are present.

The close agreement between the finite difference and analytic solutions displayed in Fig. 3 is all the more remarkable because E_y is a derived field, i.e. it is obtained from B_x, the component actually calculated in the finite difference method, by a process which is equivalent to numerical differentiation. In order to compare values of B_x (and also values of the other electric field component E_z), it is necessary to go to the interior of the conductor. In Fig. 4 the variations of B_x, E_y and E_z along the plane $z = 15$ km are depicted. This time only the finite difference results are plotted alongside the analytic solutions because it is not possible, without modifying the program, to obtain fields inside the conductor using the finite element program supplied by Kisak and Silvester. Once again excellent agreement between the analytical and numerical results is obtained.

Unfortunately it is not possible to find a similar analytic solution of the control model for an E-polarisation field. This is because no similar boundary condition corresponding to $B_x(y,0)=B_o$ exists on the surface of the conductor in E-polarisation. The method of successive approximations proposed by Weidelt (1966) and developed by Klügel (1976,1977) and Rodemann (1978), is based on the more complicated boundary condition

$$B_y(y,0) = B_o - K\, B_z(y,0) \qquad (2)$$

where K is the Kertz operator (or negative Hilbert transform) defined by

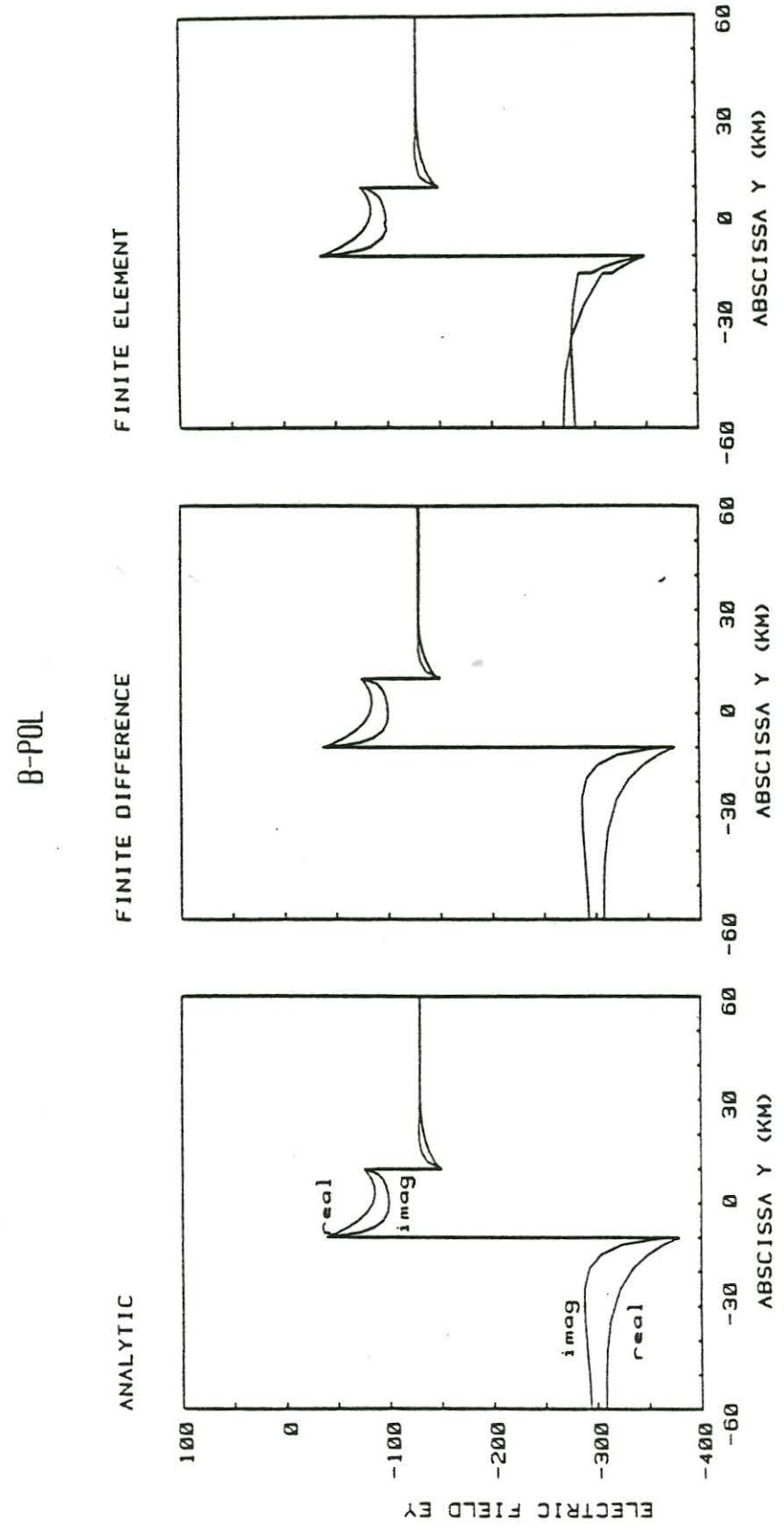
B-POL
ANALYTIC
FINITE DIFFERENCE
FINITE ELEMENT
ELECTRIC FIELD EY
100
0
-100
-200
-300
-400
real
imag
imag
real
-60
-30
0
30
60
ABSCISSA Y (KM)

Fig. 3

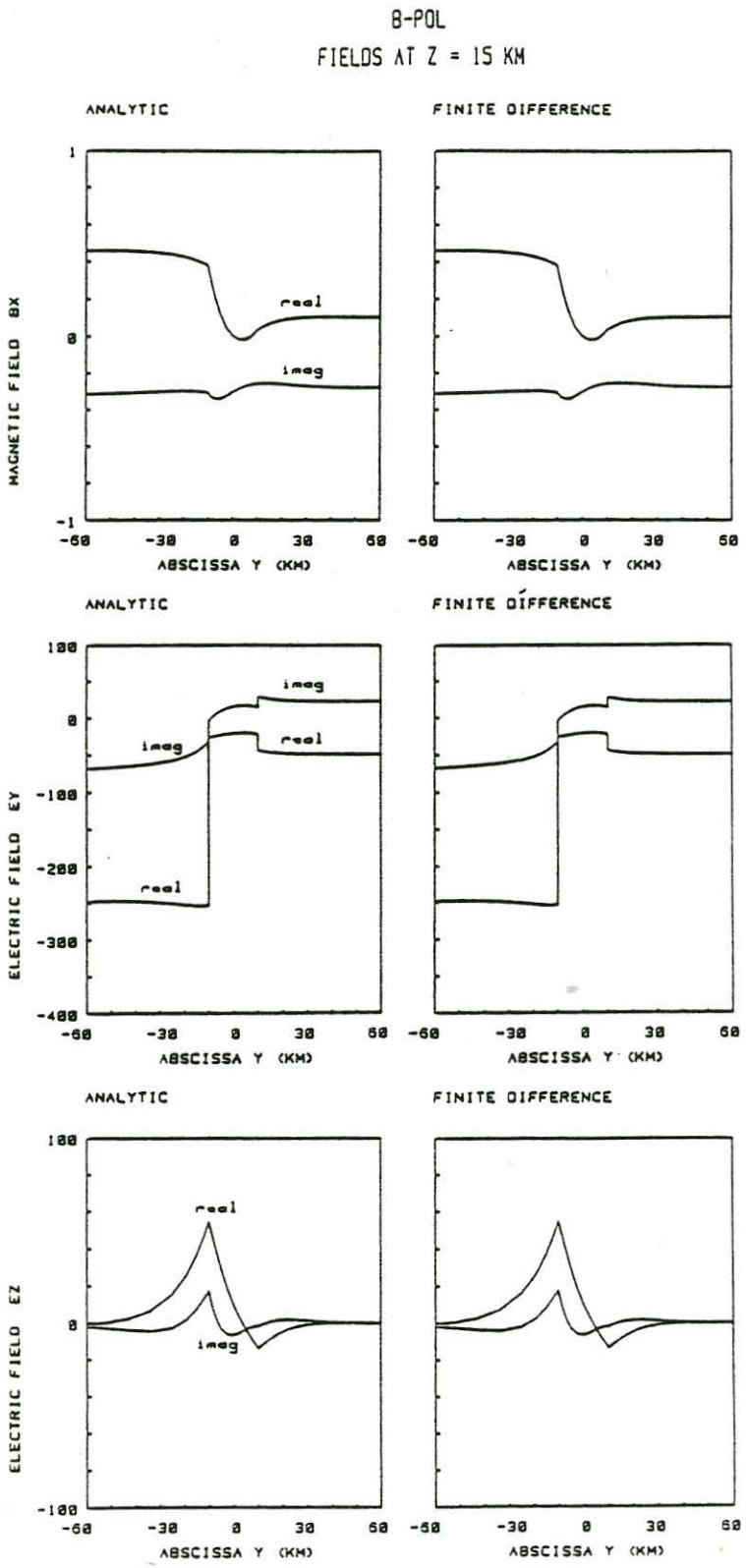
B-POL
FIELDS AT Z = 15 KM
ANALYTIC
FINITE DIFFERENCE
MAGNETIC FIELD BX
real
imag
ABSCISSA Y (KM)
ELECTRIC FIELD EY
ELECTRIC FIELD EZ

Fig. 4

$$Kf(y) = \frac{1}{\pi} \int_{-\infty}^{\infty} \frac{f(\eta)}{y-\eta} \, d\eta \quad .$$

Now B_z can be related to B_y by a formula of the type

$$B_z(y,0) = - \int_{-\infty}^{\infty} \Gamma(y,v) \, B_y(v,0) \, dv \quad ,$$

where the kernel Γ is a function that can be calculated analytically for the control model in question. In conjunction with (2) this leads to Weidelt's scheme

$$B_y^{[0]}(y,0) = B_o \quad , \tag{3}$$

$$B_y^{[N+1]}(y,0) = B_o + \frac{1}{\pi} \int_{-\infty}^{\infty} \frac{d\eta}{y-\eta} \int_{-\infty}^{\infty} \Gamma(\eta,v) \, B_y^{[N]}(v,0) \, dv \quad , \tag{4}$$

which gives $B_y(y,0) = \lim_{N\to\infty} B_y^{[N]}(y,0)$ provided that this sequence converges.

If we define

$$\Delta^{[N]}(y) = B^{[N]}(y,0) - B^{[N-1]}(y,0)$$

then the scheme can be recast in the form

$$\Delta^{[0]}(y) = B_o \quad , \tag{5}$$

$$\Delta^{[N+1]}(y) = \frac{1}{\pi} \int_{-\infty}^{\infty} \frac{d\eta}{y-\eta} \int_{-\infty}^{\infty} \Gamma(\eta,v) \, \Delta^{[N]}(v) \, dv \quad , \tag{6}$$

with

$$B_y(y,0) = \sum_{N=0}^{\infty} \Delta^{[N]}(y) \tag{7}$$

if this sum converges. The form of the scheme defined by (5), (6) and (7) is the method of successive approximations proposed independently by Mann (1970). Once $B_y(y,0)$ has been found the other components can be calculated with the aid of the appropriate Green's functions.

We have actually chosen to proceed with the iteration in a somewhat different manner. It turns out that

$$h(y) = \frac{1}{\pi} \int_{-\infty}^{\infty} \frac{d\eta}{y-\eta} \int_{-\infty}^{\infty} \Gamma(\eta,v)\, dv = \frac{1}{\pi} \int_{-\infty}^{\infty} dv \int_{-\infty}^{\infty} \frac{\Gamma(\eta,v)}{y-\eta}\, d\eta \qquad (8)$$

can be evaluated analytically in terms of the exponential integral function so that we may write

$$B_y^{[1]}(y,0) = B_o\{1 + h(y)\} \ . \qquad (9)$$

for the first approximation to the horizontal magnetic field. In fact for the special cases of the two-plate ($\sigma_2 = \sigma_3$, $y' = y + a$) and quarter-space ($\sigma_2 = \sigma_3$, $y' = y + a$, $d \to \infty$) models, (9) reduces to the analytic solutions found by Treumann (1970) and Weaver and Thomson (1972) respectively. If we now add and subtract $h(y)B_y^{[N]}(y,0)$ on the right side of (4), using the integral expression on the right of (8) for the term subtracted, and then interchange the order of integration in the repeated integral in (4), we obtain for $N \geq 1$

$$B_y^{[N+1]}(y,0) = B_o + h(y)B_y^{[N]}(y,0) + \int_{-\infty}^{\infty} \Xi(v,y)\{B_y^{[N]}(v,0) - B_y^{[N]}(y,0)\}dv \qquad (10)$$

where

$$\Xi(v,y) = \frac{1}{\pi} \int_{-\infty}^{\infty} \frac{\Gamma(\eta,v)}{y-\eta}\, d\eta \quad , \qquad (11)$$

which can be evaluated analytically (again in terms of the exponential integral) for the particular control model under investigation. The subtraction of magnetic fields in the integral in equation (10) effectively removes a logarithmic singularity in the integrand at $v = y$ that would otherwise obtain. Equations (9) and (10) define the iteration scheme we use.

The actual derivation of the analytic expression for evaluation of (11), and the handling of the integral operator in (10) involves a considerable amount of complicated algebra, which it is not our intention to reproduce here. Work is currently in progress on the completion of the computer program to compute $B_y(y,0)$ by this method.

Even though the analytic control solutions are not yet available we have undertaken a preliminary comparison of the E-polarisation finite difference and finite element calculations for the same model (Fig. 1b). Since asymptotic boundary conditions (Weaver and Brewitt-Taylor, 1978) can be used in the finite difference method, ten fewer nodes were needed in the horizontal direction (the points actually used are the same as those listed previously from y = -61 km to y = 30 km inclusive), but the grid had to be extended upwards into the air region with additional nodes at z = -1.5, -3, -5, -8, -12, -17, -25, -37, -50 and -65 km, making the total dimensions of the grid 25 x 26. For the finite element calculations the triangulation of the entire region as shown in Fig. 2 was used. Only one strip of triangular elements in the air is shown. The program of Kisak and Silvester automatically adds identical strips above it to cover the region $z < 0$. In our calculations a total of three such strips were specified, each of thickness 30 km or approximatively 1 skin-depth of the left segment in the conductivity plate. Fig. 5 depicts the variation of the real and imaginary parts of the horizontal electric field E_x across the surface of the conductor as given by the finite difference and the finite element calculations. Very good agreement, especially in the real parts, between the two methods is observed for $y < 0$, but the two sets of curves begin to diverge as y increases through positive values. The same phenomenon can be seen in the corresponding variations of the horizontal magnetic field B_y shown in Fig. 6. The general agreement between the calculated values of the vertical magnetic field B_z, also shown in Fig. 5, is not so close and in fact the finite element curve fails to reproduce the cusp-like variation at the boundary $y = \pm 10$ km. However as $|y| \to \infty$ both sets of curves are converging to zero as required.

In order to examine the differences in E_x for positive y in more detail the calculations were repeated on a much larger grid extending from y = -700 km to y = +700 km and for a larger conductivity contrast obtained by putting $\sigma_3 = 0.001$ S/m. Figs. 7(a) and (b) show that as $y \to \infty$, E_x tends to quite different values

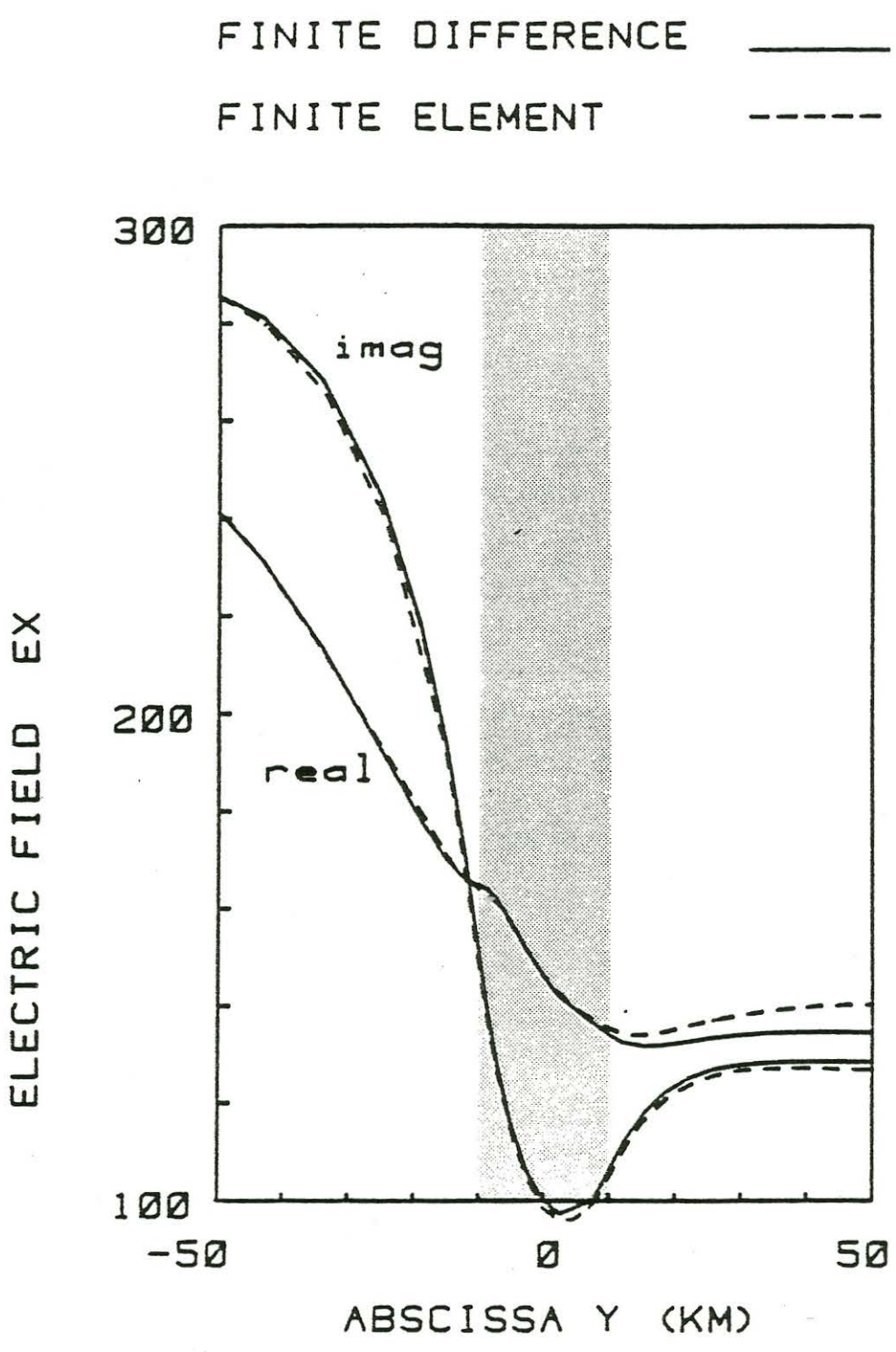
FINITE DIFFERENCE
FINITE ELEMENT
300
200
100
imag
real
ELECTRIC FIELD EX
-50
0
50
ABSCISSA Y (KM)

Fig. 5

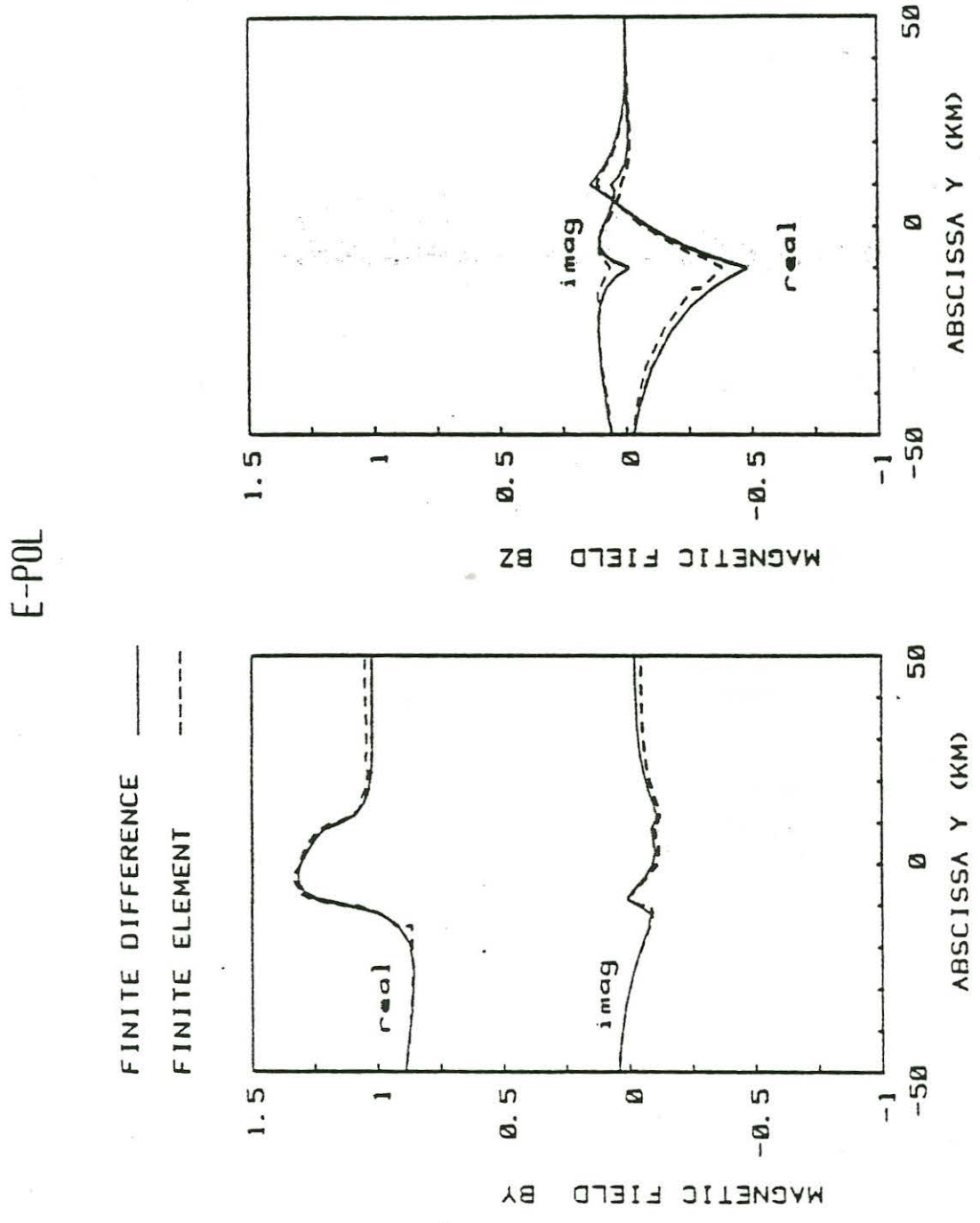
E-POL
FINITE DIFFERENCE
FINITE ELEMENT
real
imag
MAGNETIC FIELD BY
MAGNETIC FIELD BZ
ABSCISSA Y (KM)
1.5
1
0.5
0
-0.5
-1
-50
0
50

Fig. 6

E-POL

ELECTRIC FIELD EX

(a) FINITE DIFFERENCE

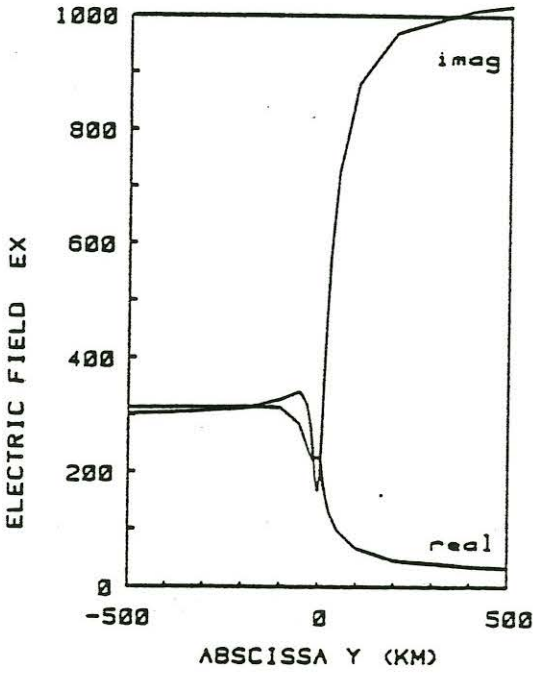

(b) THIN AIR STRIP
FINITE ELEMENT

(c) THICK AIR STRIP
FINITE ELEMENT

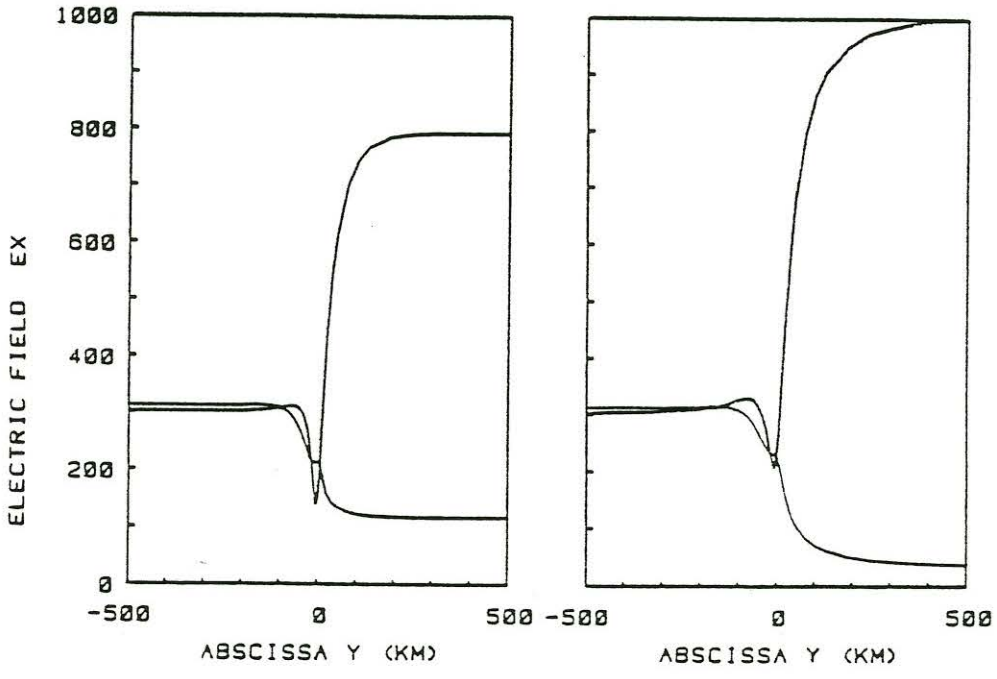

Fig. 7

depending on whether the finite difference or the finite element method is used, the discrepancy being as much as 20%. We attribute this error to the fact that Kisak and Silvester make the (false) assumption that E_x is constant across the top of their grid whereas at height h it should in fact change smoothly from its (one-dimensional) value $i\omega B_o[\tanh(d\alpha_1\sqrt{i})/\alpha_1\sqrt{i} - h]$ on the left hand side to $i\omega B_o[\tanh(d\alpha_3\sqrt{i})/\alpha_3\sqrt{i} - h]$ on the right. Only if $\sigma_1 = \sigma_3$ or if h is very large (so that it dominates $\tanh(d\alpha_1\sqrt{i})/\alpha_1\sqrt{i}$ and $\tanh(d\alpha_3\sqrt{i})/\alpha_3\sqrt{i}$) will the assumed condition of constant E_x be approximately valid. Similar errors are found for y large and positive in the values of B_y calculated by the finite element method but they tend to cancel out when the field ratio E_x/B_y is taken, so that the program still gives reasonably accurate values of apparent resistivity and phase on the right hand edge of the model. It is clear, therefore, that apparent resistivity is not a reliable indicator of the accuracy of a numerical method; it is important that actual field values are used when comparing the accuracy of different modelling programs.

Finally, the finite element calculations were repeated with the top of the grid at a sufficiently great height h that Kisak and Silvester's assumed boundary condition there is approximately fulfilled. This was done by taking the thickness of each strip of triangular elements in the air to be 300 km rather than 30 km, i.e. about 1 skin-depth of the right rather than the left segment. It can be seen from Fig. 7c that this does indeed correct the value of E_x on the right but only at the expense of introducing numerical inaccuracies near the centre of the grid caused by underflow. This arises because with such a thick strip the triangular elements near y = 0 – where the density of horizontal points is greatest – become extremely thin and elongated. As a result the minimum in the curve for Im E_x at y = 0 is shifted by about 15%, while the effect on the magnetic fields (not shown here) is even more serious with fictitious bumps appearing on the curves depicting the variation near the origin.

We conclude that the finite element program of Kisak and Silvester cannot cope with models which have different one-dimensional

structures at $y = \pm\infty$. The finite difference program of Brewitt-Taylor and Weaver appears to be quite reliable in such cases, but we must wait for the completion of our investigation of the quasi-analytic solution before we can estimate its accuracy in E-polarisation calculations with confidence.

References:

Brewitt-Taylor, C.R. and Weaver, J.T., 1976. On the finite difference solution of two-dimensional induction problems, Geophys. J. R. astr. Soc. 47, 375-396.

d'Erceville, I. and Kunetz, G., 1962. Some observations regarding naturally occuring electromagnetic fields in applied geophysics, Geophysics 27, 651-665.

Kisak, E. and Silvester, P., 1975. A finite element program package for magnetotelluric modelling, Comp. Phys. Comm., 10, 421-433.

Klügel, M., 1976. Berechnung der elektromagnetischen Induktion in zwei Halbplatten zur Anwendung in der Magnetotellurik und erdmagnetischen Tiefensondierung, Diplomarbeit, Braunschweig, Techn. Univ., Inst. Geophys. Meteorol. .

Klügel, M., 1977. Induction in plates with two-dimensional conductivity distribution, Acta Geodaet., Geophys. et Montanist. Acad. Sci. Hung. 12, 267-273.

Losecke, W. and Müller, W., 1975. Two-dimensional magnetotelluric model calculations for overhanging, high resistivity structures, J. Geophys., 41, 311-319.

Mann, J.E., 1970. A perturbation technique for solving boundary value problems arising in the electrodynamics of conducting bodies, Appl. Sci. Res. 22, 113-126.

Rodemann, H., 1978. Elektromagnetische Induktion in einer Leitfähigen Platte mit eingelagertem vertikalem, endlichem Zylinder, Dissertation, Braunschweig, Techn. Univ., Inst. Geophys. Meteorol. (Gamma 30, pp. 188).

Treumann, R., 1970. Electromagnetic induction problem in plates with two-dimensional conductivity distribution: II. Approximate method and solutions, Geomagn. Aeronom. 10, 464-472.

Wait, J.R., 1982. Geo-electromagnetism, Academic Press, New York, pp. 197-201.

Wait, J.R. and Spies, K.P., 1974. Magneto-telluric fields for a segmented overburden, J. Geomag. Geoelectr. 26, 449-458.

Weaver, J.T. and Brewitt-Taylor, C.R., 1978. Improved boundary conditions for the numerical solution of E-polarisation problems in geomagnetic induction, Geophys. J.R. astr. Soc. 54, 309-317.

Weaver, J.T. and Thomson, D.W., 1972. Induction in a non-uniform conducting half-space by an external line current, Geophys. J.R. astr. Soc., 28, 163-185.

Weidelt, P., 1966. Modellrechnungen zur Deutung der norddeutschen Leitfähigkeitsanomalie als oberflächennahe Leitfähigkeitsänderung, Diplomarbeit, Univ. Göttingen.

Ackowledgments:

This work was supported by grants from the Swiss Natural Sciences Foundation and the Geophysical Commission of the Academy of Natural Sciences. It was undertaken while one of us (J. T. W.) was spending a 6-month leave from the University of Victoria (B. C., Canada) at the Observatoire Cantonal de Neuchâtel. Financial support from the Swiss Natural Sciences Foundation and the Canton of Neuchâtel, which made this stay possible, is gratefully acknowledged. J. T. W. would also like to thank Gaston Fischer and his colleagues for their very kind hospitality during his visit.